

1 **Plants face the flow in V-formation: a study of plant patch alignment in streams**

2 Authors:

3 Loreta Cornacchia^{1,7, a} loreta.cornacchia@nioz.nl, loreta.cornacchia@univ-lyon1.fr
4 Andrew Folkard² a.folkard@lancaster.ac.uk
5 Grieg Davies³ grieg.davies@southernwater.co.uk
6 Robert C. Grabowski⁴ r.c.grabowski@cranfield.ac.uk
7 Johan van de Koppel^{1,7} johan.van.de.koppel@nioz.nl
8 Daphne van der Wal^{1,8} daphne.van.der.wal@nioz.nl
9 Geraldene Wharton⁵ g.wharton@qmul.ac.uk
10 Sara Puijalon⁶ sara.puijalon@univ-lyon1.fr
11 Tjeerd J. Bouma^{1,7} tjeerd.bouma@nioz.nl

12 Affiliations:

14 ¹ NIOZ Royal Netherlands Institute for Sea Research, Department of Estuarine and Delta
15 Systems, and Utrecht University, P.O. Box 140, 4400 AC Yerseke, the Netherlands.

16 ² Lancaster Environment Centre, Lancaster University, Lancaster, UK

17 ³ Southern Water Services, Southern House, Worthing, UK

18 ⁴ Cranfield Water Science Institute, Cranfield University, Cranfield, UK

19 ⁵ School of Geography, Queen Mary University of London, London, UK

20 ⁶ Univ Lyon, Université Claude Bernard Lyon 1, CNRS, ENTPE, UMR 5023 LEHNA, F-69622,
21 Villeurbanne, France

22 ⁷ Groningen Institute for Evolutionary Life Sciences, University of Groningen, PO Box 11103,
23 9700 CC Groningen, The Netherlands

24 ⁸ Faculty of Geo-Information Science and Earth Observation (ITC), University of Twente, P.O.
25 Box 217, 7500 AE Enschede, The Netherlands

26 ^a Present address: UMR 5023 LEHNA, Université Lyon 1, CNRS, ENTPE, Villeurbanne Cedex,
27 France

28 Corresponding author:

29 Loreta Cornacchia
30 NIOZ Royal Netherlands Institute for Sea Research
31 Korringaweg 7
32 4401 NT Yerseke
33 The Netherlands
34 email: loreta.cornacchia@nioz.nl
35 Tel.: +31 (0)113 577 457
36 Fax: +31 (0)113 573 616

37

38 Running head: Plant patch alignment in streams

39 Keywords: *submerged aquatic macrophytes; spatial patterning; eco-hydrodynamics; bio-physical*
40 *feedbacks*

41 **Abstract**

42 Interactions between biological and physical processes, so-called bio-physical feedbacks, are
43 important for landscape evolution. While these feedbacks have been quantified for isolated patches
44 of vegetation in aquatic ecosystems, we still lack knowledge of how the location of one patch
45 affects the occurrence of others. To test for patterns in the spatial distribution of vegetation patches
46 in streams, we first measured the distance between *Callitriche platycarpa* patches using aerial
47 images. Then, we measured the effects of varying patch separation distance on flow velocity,
48 turbulence, and drag on plants in a field manipulation experiment. Lastly, we investigated whether
49 these patterns of patch alignment developed over time following locations of reduced
50 hydrodynamic forces, using two-year field observations of the temporal patch dynamics of
51 *Ranunculus penicillatus* in a lowland chalk stream. Our results suggest that vegetation patches in
52 streams organize themselves in V-like shapes to reduce drag forces, creating an optimal
53 configuration that decreases hydrodynamic forces and may therefore encourage patch growth.
54 Downstream patches are more frequently found at the rear and slightly overlapping the upstream
55 patch, in locations that are partially sheltered by the established upstream vegetation while ensuring
56 exposure to incoming flow (important for nutrient availability). Observations of macrophyte patch
57 dynamics over time indicated that neighbouring patches tend to grow in a slightly angled line,
58 producing a spatial pattern resembling the V-formation in migratory birds. These findings point to
59 the general role of bio-physical interactions in shaping how organisms align themselves spatially to
60 aero- and hydrodynamic flows at a range of scales.

61 **Introduction**

62 Biogeomorphic landscapes, such as rivers, mangroves and salt marshes, are characterized by strong
63 interactions between biological and physical processes. These reciprocal interactions, also referred
64 to as bio-physical feedbacks, are fundamental for landscape formation, adjustment, and evolution
65 (Corenblit et al. 2007; Murray et al. 2008; Corenblit et al. 2015). By obstructing the flow,
66 vegetation stimulates channel formation in tidal marsh landscapes (Temmerman et al. 2007;
67 Kearney and Fagherazzi 2016). In fluvial environments, riparian and floodplain plants affect the
68 processes and morphology of alluvial rivers (Tal and Paola 2007; Gurnell 2014). Such
69 environments are characterized by the presence of ecosystem engineers (Jones et al. 1994; Gurnell
70 2014), organisms that are able to modify their habitat through their action or their own physical
71 structure or actions. To understand these biogeomorphic systems, many studies have focused on
72 interactions between vegetation, hydrodynamics, and sedimentation processes (Leonard and Luther
73 1995; Madsen et al. 2001; Bouma et al. 2007). These landscapes are often characterised by patchy
74 vegetation, at least during the establishment phase. However, despite many plants being the
75 keystone species in these environments, understanding of how flow modification at the patch scale
76 may affect the processes and mechanisms controlling vegetation establishment and the
77 hydrodynamics of these systems remains limited.

78 The interactions between flowing water and plants have been studied across different
79 ecosystems, over a variety of spatial scales and vegetation configurations. Such configurations
80 include homogeneous fields of vegetation (Kouwen and Unny 1973; Nepf and Vivoni 2000; Chen
81 et al. 2013) as well as isolated plant patches (Sand-Jensen and Vindbæk Madsen 1992; Bouma et al.
82 2009; Zong and Nepf 2012). The impact of a vegetation patch on hydrodynamics and sediment
83 dynamics is location and scale-dependent (Rietkerk and Van de Koppel 2008; van Wesenbeeck et

84 al. 2008; Schoelynck et al. 2012), for instance changing from reduced flow velocities within the
85 vegetation to increased velocities around it. Many more studies have been carried out on individual
86 patches of submerged aquatic macrophytes (for example, Sand-Jensen and Mebus, 1996; Sand-
87 Jensen, 1998; Sukhodolov and Sukhodolova, 2009), compared to studies with multiple macrophyte
88 stands (Cotton et al. 2006; Wharton et al. 2006; Marjoribanks et al. 2017). As patches in a
89 landscape rarely grow in isolation but rather in mosaics (Temmerman et al. 2007; Van der Wal et al.
90 2008), including a pseudo-braided pattern in rivers (Dawson 1989), one patch may affect other
91 patches by altering its local environment. The size of the gap between vegetation patches can be
92 influenced by current velocity (Fonseca and Bell 1998) and turbulence, and has implications for
93 physical and ecological processes (e.g. sedimentation, nutrient availability) (Folkard 2005; Folkard
94 2011). Recent attention has been focused on the larger-scale impact of multiple patches, and how
95 their size and/or alignment affects flow patterns (Folkard 2005; Vandenbruwaene et al. 2011;
96 Adhitya et al. 2014) and sediment deposition (Meire et al. 2014), and the implications for landscape
97 adjustments and evolution (Kondziolka and Nepf 2014; De Lima et al. 2015; Gurnell and
98 Grabowski 2016). However, knowledge is still lacking on how the location of one patch may affect
99 the occurrence of another patch, potentially leading to optimal spatial configurations due to
100 hydrodynamic force reduction.

101 Several studies have revealed the importance of facilitation, i.e. positive interactions
102 between species that promote establishment by mediation of physical stress (Bruno et al. 2003;
103 Callaway 2007). Thus, positive feedbacks created by one patch may extend beyond the patch itself
104 (Bruno and Kennedy 2000), leading to a facilitative effect on the establishment or growth of other
105 species. Such interactions between vegetation patches are likely to be relevant for plant
106 establishment in lotic environments, where primary colonization is challenging due to forces that

107 act to dislodge seedlings and fragments (Riis 2008; Balke et al. 2014). However, studies of
108 facilitation mostly focus on interactions between individuals of different species or interspecific
109 interactions (Bruno et al. 2003; Callaway 2007). Consequently, we know relatively little about
110 intraspecific facilitation mediated by existing vegetation patches of the same species and its effects
111 on distribution patterns in the landscape. It is important to address this gap as intraspecific
112 facilitation is likely to be a key process in flow-dominated systems, where currents and drag forces
113 may impose a stress that limits growth and seedling establishment (Schutten et al. 2005; Puijalon et
114 al. 2008; Balke et al. 2011). It is known that vegetation patches may increase flow velocity in some
115 adjacent areas, while reducing it directly downstream of the patch (Bouma et al. 2007; Chen et al.
116 2012; Schoelynck et al. 2012). As a consequence, optimal spatial configurations of vegetation
117 patches might be expected to emerge due to patterns of hydrodynamic force reduction, specifically
118 in terms of drag force reduction.

119 Plant-flow interactions have been studied intensively in vegetated streams because of their
120 ecological and geomorphological importance (Gurnell 2014; Bertoldi et al. 2015; Grabowski and
121 Gurnell 2016), and the presence of unidirectional flow makes them an ideal model system. In this
122 study, we investigated the spatial distribution of submerged aquatic vegetation patches and the
123 implications of this for in-stream landscape adjustments over a two-year timescale. There were
124 three components to the study. First, naturally occurring macrophyte patches were identified from
125 aerial images to determine the average patch separation distances. Then, a field manipulation
126 experiment was conducted to measure the effects of varying patch separation distance on flow
127 velocity, turbulence, and drag on the submerged plants. We considered drag reduction as a proxy
128 for the benefits derived by plants from their location in relation to other patches. Previous studies
129 indicate that, on a short temporal scale, the survival and establishment of individual plants depend

130 on successful root development (in the order of days; Barrat-Segretain et al. (1998); Barrat-
131 Segretain et al. (1999)) and protection from scouring or dislodgement due to currents and drag.
132 Most of this primary colonization phase derives from drifting vegetative fragments, and rarely from
133 seeds (Sand-Jensen et al. 1999; Riis 2008). To test whether the most frequent patch distributions
134 corresponded to the locations with the lowest drag forces, we related patterns of drag reduction to
135 the observed probability of patch occurrence identified from aerial images. After colonization,
136 single shoots develop into patches on intra-annual time scales through clonal expansion (over the
137 course of months; Cotton et al. (2006); Wharton et al. (2006)). Therefore, finally we tested whether
138 such preferential patch distributions obtained from aerial images were supported by field
139 observations of temporal patch dynamics in a lowland chalk stream over a period of two years.

140 **Materials and methods**

141 **Measuring inter-patch distance from in-stream aerial images**

142 To investigate the existence of preferential distributions of plant patches, we collected aerial images
143 of an artificial drainage channel with natural colonization by aquatic vegetation. The channel is
144 located along the Rhône River (France), near Serrières-de-Briord (45.8153 ° N, 5.4274 ° E). The
145 channel, selected for its uniform cross-sectional and planform geometry allowing a focus on plant
146 configuration, had an average channel width of 8.0 m, an average depth of 0.8 m, rarely exceeding
147 1.3 m, with relatively straight banks. Aerial images of the streambed were taken with a digital
148 camera mounted on a pole at a height of c. 2 m. We identified 22 pairs of neighbouring patches for
149 the dominant aquatic macrophyte *Callitriche platycarpa*. This species has long, flexible shoots that
150 are pushed in a downstream direction by the flow, generating an overhanging canopy that is rooted

151 only at the upstream edge (Haslam 1978). The pairs could clearly be distinguished as separate
152 patches through the presence of an unvegetated area between their rooting parts. In these streams,
153 neighbouring patches were defined as those within 1.5 m from each other, because the influence of
154 an upstream patch can be observed for a distance equal to its length (Sand-Jensen and Mebus 1996;
155 Schoelynck et al. 2012), and 1.5 m is representative of the average length of *C. platycarpa* patches
156 (Sand-Jensen 1998). We measured the absolute longitudinal inter-patch distance (distance between
157 their upstream edges in the streamwise direction, L_d in m) and transversal inter-patch distance
158 (distance between their leftmost edges in the spanwise direction, T_d in m) between the pairs (Figure
159 1). To account for differences in absolute distances due to the variability in patch sizes, we
160 converted them into relative distances. To obtain relative longitudinal distances (L), we divided the
161 absolute distance L_d by the length of the upstream patch L_u . To obtain relative transversal distances
162 (T), we divided the absolute distance T_d by the width of the upstream patch T_u (Figure 1). The
163 frequency distributions of relative longitudinal and transversal distances were first converted into
164 probability distributions. Then, the probability distributions in the two directions were multiplied by
165 each other to obtain the probability of naturally-observed occurrences of vegetation patches for
166 each combination of L and T distances. This point grid was imported into GIS software and
167 interpolated to obtain a two-dimensional probability map of naturally-observed patch occurrence
168 (%) at different distances from an existing patch, using kriging interpolation.

169 **Quantifying the effects of inter-patch distance on flow velocity and drag using a field** 170 **manipulation experiment**

171 Flow velocity measurements

172 To assess the effects of different patch configurations on flow reduction and acceleration, we
173 measured the changes in flow velocity with varying patch separation distance through a field
174 manipulation. Plants were detached from existing patches, transplanted on perforated metal plates
175 and fixed through cable ties at the roots, to recreate two *C. platycarpa* patches (1.2 m in length, 0.6
176 m in width) that could be moved and arranged at different distances in the river bed. The two
177 patches were arranged into 10 different configurations, representing a combination of longitudinal
178 and transversal distances (Figure 2). The patch located upstream (“patch U”) was kept fixed, while
179 the other one (“patch D”) was moved downstream and/or laterally to create the configurations. The
180 two patches were partially overlapping in one configuration ($T = 0.5$, $L = 0.46$), as the leading edge
181 of patch D started at the end of the rooted area of patch U. In this case, the overhanging canopy of
182 patch U was located in the upper water layer, while the leading edge of patch D was located close
183 to the bed, which still allowed water to flow in between the two patches. The patch characteristics
184 (width, length and density) were kept constant between the fixed and mobile patches. Patch density
185 was fixed by fitting the plants into the perforated metal plates, with an array of 9408 holes per m^2 .
186 The condition of the plant patches did not deteriorate during the course of the experiment, thus
187 maintaining a similar morphological function within the river.

188 Vertical profiles of flow velocity were measured with a 3D acoustic Doppler velocimeter
189 (ADV, Nortek) over 2 min at 10 Hz. Hydrodynamic profiles were measured at five vertical
190 locations of 5, 10, 20, 40 and 90% of the depth above the river bed. Around the pair of vegetation
191 patches, vertical profiles were located at distances of 0.2 m and 0.1 m respectively from the
192 upstream edges, and 0.2 m on both sides of each patch (at 0.35 m along their length), i.e. in the gap
193 between the patches. For each point measurement in the profile, mean values of the velocity
194 components u , v and w were calculated (corresponding to velocities in the x , y and z directions; $m\ s^{-1}$).
195 Depth-averaged flow velocities u (in the streamwise direction) are expressed relative to

196 incoming flow velocity, which was recorded at a fixed measurement point located 0.5 m upstream
197 of patch U.

198 Turbulent kinetic energy

199 To determine the effects of different patch configurations on turbulence, we measured the changes
200 in turbulent kinetic energy (TKE, $\text{m}^2 \text{s}^{-2}$) with different patch separation distances. TKE is a
201 measure of hydrodynamic turbulence that can negatively affect plants through direct effects on their
202 growth (Jaffe and Forbes 1993). Also, by governing processes of sediment trapping and
203 resuspension (Hendriks et al. 2008), it can potentially affect plant establishment by reducing
204 sediment stability. TKE was therefore calculated for the profile located at 0.1 m from the upstream
205 edge of patch D, to investigate its potential implications for establishment. We first calculated the
206 turbulent fluctuations $u'(t) = u(t) - \bar{u}$ where $u(t)$ is the time series of flow measurements and \bar{u}
207 is the time-averaged velocity (m s^{-1}) in the streamwise direction at each vertical position. The
208 corresponding spanwise and vertical turbulent velocity components v' and w' were calculated in
209 the same way. For each point measurement in the profile, turbulent kinetic energy (per unit mass)
210 was then calculated as $TKE = \frac{1}{2} (\overline{u'^2} + \overline{v'^2} + \overline{w'^2})$.

211 Drag force measurements

212 To investigate the benefits of different patch configurations in terms of drag reduction, we
213 measured the effects of varying patch separation distance on drag forces. Drag forces were
214 measured using a force transducer developed by the former WL Delft Hydraulics (now Deltares,
215 Delft, The Netherlands). The transducer consisted of a solid platform, carried by two steel
216 cantilever beams, with four temperature-corrected strain gauges mounted in pairs on opposite sides
217 of each of the two steel cantilevers (for details see Bouma et al. (2005)). The voltage output for the

218 force transducer was linearly correlated with forces up to 10 N ($r^2 = 0.99$, $p < 0.001$). During the
219 measurements, a *C. platycarpa* plant was mounted on top of the transducer and placed into the river
220 bed at the upstream edge of patch D. For the measurements, we selected isolated plants of $55.1 \pm$
221 5.8 cm in height and with 4 to 9 ramifications. Plants were attached to the transducer by their stem,
222 and positioned in a natural growth position to closely represent the natural conditions. Voltage
223 readings were collected on a data logger at a frequency of 100 Hz and expressed as the mean value
224 for 1 min. As bending and leaning of the plant on the vegetation patch interferes with measuring the
225 actual drag on the individual, drag measurements were also performed by removing patch D and
226 repeating the measurement on the single plant. To allow comparisons between individuals, drag
227 was expressed as a function of total plant surface area.

228 **Effects of patch interactions on seasonal in-stream landscape adjustments: evidence from** 229 **temporal field surveys**

230 To test whether new vegetation occurred preferentially at certain distances and directions from
231 initial vegetation patches, we analysed field surveys of vegetation development from a study on a
232 chalk stream reach within the Frome-Piddle catchment (Dorset, UK) over two years (monthly from
233 July 2008 to July 2009, and bimonthly thereafter until July 2010; for further information on the
234 field surveys, please see Davies (2012)). The study reach was the Bere Stream (UK Grid Reference
235 385563, 93009), a relatively straight 30 m section with bankfull widths ranging between 7-9 m. The
236 dominant in-channel aquatic macrophyte was water crowfoot (*Ranunculus penicillatus* subsp.
237 *pseudofluitans*) which has highly similar patch establishment dynamics and structural traits to
238 *Callitriche platycarpa* (rooted at the upstream part of the patch and with very flexible stems that
239 form an overhanging canopy; Haslam 1978). Furthermore, the main factors affecting initial

240 establishment are determined by mechanical forces (e.g. drag, flow velocity). These forces increase
241 the risk of plant uprooting or dislodgement and relate to plant morphological characteristics (Bal et
242 al. 2011), rather than species characteristics such as growth rates. Thus, field observations of
243 *Ranunculus* could be compared with the findings of the field manipulation experiments of *C.*
244 *platycarpa*.

245 The data set from the Frome-Piddle catchment afforded a unique opportunity to assess the
246 occurrence of new vegetation and changes in vegetation cover and spatial distribution over time.
247 The field survey was a repeated measures design over time. During each survey, macrophyte
248 distribution was mapped along 30 transects that were located at 1-m distance intervals along the 30-
249 m long study reach. Along each transect, measurement points were located at 0.5 m intervals to
250 record macrophyte presence and species. The sample size was 2150 measurement points, replicated
251 over 19 surveys, of which six surveys were used in this study. Reach survey data were analysed
252 using GIS software. The total station coordinates of the transect markers were used to georeference
253 a digitised version of the reach within a GIS. The output resulted in an array of points that were
254 spatially arranged along transect lines. Vegetation cover observed at points in the reach data set
255 were interpolated using an Inverse Distance Weighted (IDW) interpolation method. If the predicted
256 surface outputs from IDW differed from the substrate cover observed at any extra observation point
257 not used in the IDW, the substrate cover observed at that point prevailed above the IDW
258 interpolation. Separate vegetation patches were derived using the minimum bounding geometry
259 enclosing each of the polygon outputs from IDW. Although not measured in this study, seasonal
260 changes in macrophyte cover are generally associated with changes in vegetation biomass density
261 (g dry weight m⁻²). A previous study in the Bere Stream found that *Ranunculus* density was lowest
262 during winter (January, about 100 g DW m⁻²) and peaked during the summer months (May – July),
263 when it reached about 400 g DW m⁻² (Dawson 1976).

264 We tested the hypothesis that directions of growth of new patches compared to existing
265 patches during the survey period show preferential directions for plant growth, instead of being
266 uniformly distributed in all directions. Therefore, six replicate surveys over three different periods
267 were selected over the two years (December 2008 – July 2009, September 2009 – January 2010,
268 January 2010 – July 2010) because a net increase in *Ranunculus* cover was measured within each
269 of them, allowing the phase of new macrophyte patch colonization to be captured. The shortest
270 distance and direction (angle) between each new vegetation patch and the closest existing patch at
271 the beginning of each survey period were calculated using the ‘Near’ tool in ArcMap 10.4.

272 **Statistical analyses**

273 In the aerial photography, 22 replicate pairs of patches were considered. A chi-squared test was
274 used to test for significant differences in the frequency of observed longitudinal and transversal
275 distances between vegetation patches. In the field experiment, the statistical design was a fully
276 factorial design with transversal and longitudinal distances as the main factors, comprising ten
277 different configurations (treatments) each measured once. Regression analysis was used to test the
278 effects of varying longitudinal and transversal distances on depth-averaged and near-bed (5 and
279 10% of depth above the river bed) flow velocities in four different positions (between the patches,
280 at the upstream edge of patch D, next to patch U, next to patch D), and on turbulent kinetic energy
281 at the upstream edge of patch D. We tested whether relative flow velocities would increase linearly
282 with increasing inter-patch distances, or follow a quadratic relationship which might be expected if
283 relative flow velocities first increase until a maximum at intermediate distances, and then decrease
284 to 1 as they become equal to incoming flow velocity. In the latter case, patches become far enough
285 apart so that they cease to interact. Hence, we fitted both linear and quadratic models using single
286 (L or T distances) and multiple (L and T distances) predictor variables. We then used Akaike’s

287 Information Criterion to compare the adequacy of the candidate models, and selected the model
288 with the lowest AIC score (Akaike 1998). Regression analysis was used to test for the relationship
289 between flow velocities and drag forces on *C. platycarpa* in the field flume experiment. Ordinary
290 Least Square (OLS) regression was used for spatial regression between the experimental drag
291 measured around a vegetation patch, and the probability of naturally-observed patch occurrence.
292 The latter was first log-transformed (natural log of original value + 0.5) due to its skewed
293 distribution. A chi-squared test was used to test for significant differences in angle of growth
294 compared to a uniform distribution in all directions. A paired t-test was used to compare drag forces
295 measured on single plants to drag on plants located at the upstream edge of a vegetation patch.

296 **Results**

297 **Observed inter-patch distances between pairs of macrophytes**

298 The analysis of aerial photographs from the Rhône River study reach revealed that naturally-
299 occurring *C. platycarpa* stands display a non-random distribution relative to neighbouring patches
300 (Figure 1). We observed that the leading edge of the downstream patch was most frequently located
301 between one third and halfway along the length of the upstream patch (i.e., $L = 0.3 - 0.5$) ($\chi^2_8 =$
302 20.54 , $p = 0.008$). This longitudinal separation distance was relatively constant, regardless of the
303 size and shape of the patches we analysed (width/length ratios ranged from 0.25 to 0.83). In the
304 transversal direction, the downstream patch was most frequently located at 80% of the width of the
305 upstream patch from the latter's lateral edge (i.e. $T = 0.8$), hence partially overlapping with, and
306 sheltered by, the overhanging canopy of the patch ahead ($\chi^2_6 = 14.90$, $p = 0.021$).

307 **Effects of inter-patch distance on flow velocity and turbulence**

308 Measurements of the hydrodynamic effects of different patch configurations in the Rhône River
309 study reach showed that depth-averaged flow velocity and turbulence patterns were strongly
310 affected by the distance between patches. In between the patches, flow velocity was strongly
311 reduced when the patches were partly overlapping (i.e. for $T = 0.5$ and $L = 0.46$), but it increased
312 when a clear separation developed between patches and flow was constricted. We found a
313 significant linear relationship between flow velocities in between the patches and the relative
314 transversal (T , spanwise) distance between the patches ($F_{1,8} = 31.45$, $r^2 = 0.79$, $p < 0.001$; Figure 3a
315 – c; Table 1). When the patches were close together, with no more than a 5 cm gap ($T \leq 1.08$), flow
316 velocities between them were reduced and the pair tended to behave more like a single patch.
317 However, flow velocity accelerated when the gap between the patches, and therefore T , increased.
318 In particular, at $T = 1.58$, flow velocities between the two patches were higher than incoming
319 velocities due to flow constriction (Figure 3b).

320 We found that turbulence was minimized at intermediate distances along the length of an
321 upstream patch, while it increased both when the patches were next to each other and when one was
322 immediately downstream of the other. Turbulent kinetic energy upstream of the patch was
323 significantly related to relative longitudinal distance L through a quadratic relationship ($F_{2,7} =$
324 5.719 , $r^2 = 0.62$, $p = 0.03$), the highest TKE occurred when patches were located next to each other
325 (for $L = 0$; Figure 3d – f). From $L=0$, TKE decreased with increased relative longitudinal distance
326 until a minimum at $L = 0.66$, after which it increased again for $L > 0.66$ as it entered the high TKE
327 region in the wake of the upstream patch. This minimum TKE at $L = 0.66$ seems to be the point at
328 which there was an optimal combination of sheltering from the oncoming flow by the upstream
329 patch (which increased with L), and minimization of the high TKE region in the wake of the

330 upstream patch (which decreased with L). For the mean flow velocities upstream of patch D, results
331 of single and multiple regression showed no significant relationship with T and L distances (Table
332 1).

333 Areas of weakest flow deflection (i.e. reduced hydrodynamic forces) were found around the
334 upstream patch at intermediate longitudinal distances and, in particular, when the two patches were
335 partly overlapping. However, flow deflection increased both when the patches were next to each
336 other and when one was immediately downstream of the other. A significant non-linear (quadratic)
337 relationship was found between flow velocities next to patch U and both relative transversal (T) and
338 relative longitudinal (L) distances ($F_{4,5} = 7.931$, $r^2 = 0.90$, $p = 0.03$; Figure 3g – i; Table 1). As L
339 increased, flow velocity first decreased for intermediate distances (between 0.16 and 0.58), due to
340 weaker flow redirection around the patch. Then, it increased again to become equal to the incoming
341 flow velocity, following a quadratic relationship. As T increased, and therefore the gap between the
342 patches increased, the flow velocity increased until it was equal to the incoming flow velocity for T
343 ≥ 1.5 . However, flow velocities next to patch D showed no significant relationship with relative
344 transversal (T) and longitudinal (L) distances (Table 1).

345 Testing the relationship between patch distance and near-bed flow velocities revealed no
346 significant relationship between patch distances and velocities at 5% of the depth above the river
347 bed (Supporting Information, Table S1). A significant quadratic relationship between flow
348 velocities in between the patches and both relative transversal (T) and relative longitudinal (L)
349 distances was confirmed for flow measurements at 10% of the depth (Supporting Information,
350 Table S2).

351 **Effects of inter-patch distances on drag forces**

352 Existing vegetation patches appeared to create sheltered areas where drag was minimized, and new
353 patches were more likely to occur in these locations. Measurements of the drag force derived from
354 a plant's particular location around an existing vegetation patch revealed a significant relationship
355 between flow velocity and drag force per unit surface area on *C. platycarpa* individuals ($r^2 = 0.92$,
356 $p = 0.0001$; Figure 4a). As our field drag force measurements were in the same order of magnitude
357 as measurements performed on the same species in a laboratory flume (Puijalon et al. 2011), we
358 assert that the field set-up provided comparable and accurate measurements. Drag forces ranged
359 from 0.19 to 4.63 N m⁻², due to the flow modification by the vegetation patch, with lowest drag
360 forces right along the lateral edge of the patch, at ≥ 0.55 m from the upstream edge. This distance
361 along the length of the patch corresponded to the end of the rooted area and the start of the floating
362 canopy, with the downstream patch forming an angle of 28° relative to the upstream patch. Plotting
363 the drag in an interpolated spatial grid around a patch shows that the most frequent locations of
364 neighbouring patches based on our field observations correspond to positions with intermediate to
365 low drag forces (Figure 4b and d). Furthermore, the probability of observed patch occurrence in a
366 certain position is inversely related to the observed drag force in that position (ordinary least
367 squares spatial regression, $r^2 = 0.28$, $p < 0.0001$, Figure 4c).

368 Comparison of average drag force measurements on single plants, representing the conditions
369 of initial establishment, compared to plants located at the upstream edge of a well-established patch
370 ($n = 10$ configurations) showed that *C. platycarpa* individuals experience significantly higher drag
371 when alone (Figure 5; paired t-test, $t_{19} = -2.28$, $p = 0.03$). This observation shows that drag forces
372 on the upstream plants are mitigated by leaning onto other plants in a patch.

373 **Effects of patch interactions on seasonal in-stream landscape adjustments: evidence from** 374 **temporal field surveys**

375 Field surveys over a two year period in the Frome-Piddle catchment (UK) showed that new
376 vegetation patches occurred at specific orientations from existing vegetation patches ($\chi^2_5 = 9.20$, $p =$
377 0.1 for Dec. 2008 – July 2009; $\chi^2_5 = 12.80$, $p = 0.025$ for Sept. 2009 – Jan. 2010; $\chi^2_5 = 10.88$, $p =$
378 0.053 for Jan. 2010 – July 2010, and $\chi^2_5 = 24.34$, $p < 0.001$ for all survey periods together; Table 2).
379 Within each of the three time periods we analysed, the most common direction of growth was at
380 angles between 0 and 60° from existing patches (with a peak around 30°), in a downstream
381 direction towards the right bank with a second most common direction at angles between 120 and
382 180° , downstream towards the left bank (Figure 6; Table 2). The most common angles of growth
383 found through field surveys are consistent with the angle of 28° found through field measurements
384 and corresponding to a region where drag forces are the lowest (Figure 4). Overall, these
385 observations support the hypothesis that new patches occur in a slightly angled line with respect to
386 existing well-established patches, in locations with reduced hydrodynamic and drag forces (Figure
387 4).

388 The observed seasonal trends of in-stream vegetation growth and die-back were similar over
389 the two survey years in the Frome-Piddle catchment (Table 2; the corresponding changes in fine
390 sediment deposition within *Ranunculus* patches are reported in Davies, 2012). During both years,
391 *Ranunculus* reached its peak cover in the period May – July and began to decline shortly after (until
392 December), due to the seasonal dieback linked to increasing channel discharge and decreasing
393 daylengths and water temperatures. In September 2009, a particularly low *Ranunculus* cover was
394 observed (7%), likely related to the increase in autumn discharges. However, in-stream vegetation
395 started to recover from January onwards, when daylengths increased, with new *Ranunculus* patches
396 recolonizing the stream bed.

397 **Discussion**

398 While most studies of bio-geomorphic feedbacks have focused on isolated or already established
399 patches, our study examined the spatial configuration of patches and quantified where plant patches
400 occur in relation to one another. A key finding was that new vegetation patches in streams organize
401 themselves in V-like shapes during the establishment phase to reduce hydrodynamic and drag
402 forces. Field observations showed that patches are more likely to grow at the end of the rooted area
403 of the upstream patch, where its floating canopy starts (i.e., between one third and halfway down
404 the length of an upstream patch), and slightly off to its side (overlapping with part of their width).
405 Measurements in the field revealed that these locations correspond to areas where drag is reduced,
406 due to partial sheltering from high flow velocities and TKE by well-established vegetation patches.
407 Field manipulations supported this hypothesis, showing that mean flow velocity is reduced by
408 partially overlapping with upstream patches in the across-stream direction, and turbulence is
409 minimized when growing halfway down the length of an upstream patch in the main flow direction.
410 Flow deflection around the upstream patch is weakest when a partial V-shape is formed, suggesting
411 that additional secondary patch growth can occur on the other side of the V. These patterns of patch
412 alignment in formation resemble the formation adopted by migratory birds (Portugal et al. 2014), or
413 the drag-reducing queue formations in spiny lobsters (Bill and Herrnkind 1976). This provides
414 evidence of the role that bio-physical interactions have in shaping the way organisms position
415 themselves spatially in landscapes, in both air- and water flow, across a range of scales.

416 *Facilitative interactions within the landscape of a self-organized species*

417 The positive and negative feedbacks underlying the formation of self-organized patterns have been
418 identified for a wide range of ecosystems (Rietkerk et al. 2002; van de Koppel et al. 2005; Larsen et
419 al. 2007). At the scale of a single patch, it is well known that a positive feedback of reduced flow

420 velocities within patches is linked to a negative feedback limiting lateral growth (Bouma et al.
421 2009; Schoelynck et al. 2012). However, while positive feedbacks are generally observed at a small
422 scale within a patch (Rietkerk and Van de Koppel 2008), knowledge of the larger-scale facilitation
423 of seedling or fragment establishment by a self-organized species is limited. Our study provides a
424 first indication of establishment mechanisms operating at this larger, between-patch scale. We show
425 how an existing vegetation patch modifies flow velocities and resulting drag forces in its
426 surroundings thereby leading to positive or negative effects on the occurrence of other patches,
427 operating at a distance. Facilitative interactions within the same self-organized species, and over
428 larger scales, might therefore be an important but overlooked process determining the evolution of
429 spatial patterns over time.

430 The spacing of the vegetation patches resembles the organized spatial configurations
431 observed in other organisms. For instance, migratory birds maximize the upward motion of air from
432 the bird ahead and reduce drag due to air resistance (Lissaman and Shollenberger 1970;
433 Weimerskirch et al. 2001; Portugal et al. 2014), and fish schools adopt different spatial
434 configurations that can lead to reduced energy expenditure (Ashraf et al. 2017). Our temporal
435 observations showed preferential patch occurrence at 0 to 60° angles from existing patches, with a
436 peak around 30°. This angle is consistent with the 28° angle at which drag on the downstream patch
437 was minimized in the field manipulation. However, the regions of minimum drag force did not
438 strictly correspond to the most frequent location of patch occurrence. This discrepancy could be due
439 to the low number of drag measurement points in that location, or to processes occurring during
440 patch development (e.g. erosion of the upstream patch front and downstream displacement of
441 patches (Sand-Jensen and Vindbæk Madsen 1992), nutrient availability, etc.). The observed
442 vegetation patch configurations might involve a balance between stress reduction and nutrient

443 availability. For submerged aquatic plants, the position immediately in the wake of another patch
444 could seem equally or even more beneficial in terms of drag reduction. However, the V position
445 might be a hydrodynamic optimum to maximize drag reduction while still ensuring exposure to
446 light and delivery of nutrients by water flow. Flume experiments on nitrogen uptake showed that
447 ammonium uptake rates for *Callitriche* increased when the patch was located at a leading edge,
448 where it was exposed to higher mean velocity (Cornacchia et al. 2018a). Instead, *Callitriche* had
449 very low ammonium uptake rates when it was immediately downstream of another patch and
450 exposed to low mean velocities. This finding suggests that partial, rather than complete, sheltering
451 by established vegetation can allow more nutrients to be delivered to the downstream patch.
452 Similarly, in mussel beds, aggregation at high densities provides the advantage of protection from
453 physical forces, but also increases competition for food (van de Koppel et al. 2005; De Paoli 2017).
454 Therefore, the balance between reducing stress and maintaining resource availability might be an
455 important factor influencing patch distributions in different self-organized systems. Further
456 measurements of hydrodynamics and nutrient uptake, and/or numerical modelling studies are
457 required to investigate the physical explanation for these patterns such as the V formation.

458 The consistency between the neighbouring patch distances observed for *Callitriche*
459 *platycarpa* and *Ranunculus penicillatus* suggest that such V-shaped settlement might be typical for
460 lotic aquatic environments. Thus, it might be a general process for submerged aquatic vegetation in
461 running waters, at least for species with similar morphologies and experiencing comparable drag
462 forces (Bal et al. 2011). However, vegetation distributions can be more complex than the
463 streamlined, V-shaped patterns described here. Moderate flow velocities and uni-directional flows
464 tend to create a streamlined patch distribution, whereas a near-homogeneous plant cover would
465 emerge in streams with sustained periods of low flow velocities (Cornacchia et al. 2018b).

466 Moreover, a model accounting for interactions between neighbouring patches of emergent
467 vegetation found that wake interactions and resulting deposition patterns influence secondary patch
468 growth (De Lima et al. 2015), yielding complex distributions and not necessarily recognizable V-
469 shapes. More complex patterns in vegetation growth have also been observed in a stream with a
470 rich abundance of aquatic plant species (Cameron et al. 2013). Plant traits could also influence the
471 occurrence of recognizable V-shaped patterns. For instance, a V pattern might not be expected for
472 species showing high resistance to hydrodynamic forces (Puijalon et al. 2011), high root anchorage
473 strength (Schutten et al. 2005; Gurnell et al. 2013; Liffen et al. 2013), or relying less on areas of
474 low velocity and fine sediment deposition for their establishment and growth. Our observations
475 were not able to provide evidence of this distribution pattern in other species, which were not as
476 abundant in our field sites. Further studies are necessary to test if a clear dominant species is needed
477 to achieve this configuration, and how the presence of other species might affect the patterns and
478 spacing between patches.

479 The patches in our experiment were constructed on an array of 9408 holes per m². As a non-
480 dimensional measure of canopy density (Nepf, 2012), *Callitriche* patches have a frontal area per
481 bed area $ah = 0.200 \pm 0.035$ at the incoming flow velocity of 0.24 m s⁻¹ (Cornacchia et al. 2018a).
482 This density value is similar to other studies. Bouma et al. (2007) created patches with $ah = 0.64$. In
483 Zong and Nepf (2011), ah ranged from 0.48 to 2.52. These values fall in the dense canopy regime
484 described in Nepf (2012), corresponding to $ah > 0.1$. Therefore, the hydrodynamic patterns
485 presented in this study can generally be expected in other ecosystems with flexible submerged
486 species under dense canopy conditions and presenting similar patch structure (i.e. overhanging
487 canopies).

488 *Initial patterns control future pattern formation: implications for ecosystem resilience*

489 Our results on the role of patchiness on vegetation distribution suggest that initial vegetation
490 patterns determine where future patches occur. This creates patterns at multiple spatial scales: a
491 patch-patch scale during initial establishment, which over time leads to a pseudo-braided pattern in
492 the organization of mature patches at the reach scale, with vegetated bands separated by
493 unvegetated channels. These patterns likely develop on two different time scales. On the scale of
494 generally 1 to 10 days, primary colonization by individual shoots relies on successful root
495 development (Barrat-Segretain et al. (1998); Barrat-Segretain et al. (1999)), which allows them to
496 withstand scouring or dislodgement due to currents and drag (as in our field manipulation). After
497 primary colonization, single shoots develop into patches through clonal growth over the course of
498 months, based on our monitoring data and literature studies (Cotton et al. 2006; Wharton et al.
499 2006). Therefore, the complex self-organized patterning of stream macrophytes likely results from
500 processes interacting at different spatial and temporal scales.

501 Pattern formation at multiple scales, both spatial and temporal, has also been found to
502 increase resilience in mussel beds which are another self-organized ecosystem (Liu et al. 2014).
503 Similar to macrophytes, mussel aggregation into clumps improves their growth and offers
504 protection against hydrodynamic forces (Van de Koppel et al. 2008). Thus, the presence of a few
505 initial patches can facilitate the establishment of new patches. It might promote faster recovery
506 following disturbance events such as floods by creating a self-reinforcing state that increases the
507 resilience of lotic ecosystems. The sheltering effect presumably strengthens as the number of
508 patches increases, eventually developing into near-full vegetation cover (cf. Van der Wal et al.
509 (2008) for *Spartina* tussocks growing into a fully vegetated salt marsh). In regularly disturbed
510 ecosystems, where the hydrologic regime and flow variability are among the primary factors
511 controlling macrophyte establishment and development (Riis and Biggs 2003), this process may be

512 crucially important for vegetation recovery (Barrat-Segretain et al. 1998; Barrat-Segretain et al.
513 1999; Riis 2008). Our study suggests the general role of bio-physical interactions in shaping how
514 organisms align themselves to hydrodynamic flows in different landscapes and across multiple
515 spatial scales.

516 **Acknowledgments**

517 This work was supported by the Research Executive Agency, through the 7th Framework
518 Programme of the European Union, Support for Training and Career Development of Researchers
519 (Marie Curie - FP7-PEOPLE-2012-ITN), which funded the Initial Training Network (ITN)
520 HYTECH ‘Hydrodynamic Transport in Ecologically Critical Heterogeneous Interfaces’, N.316546.
521 Data collection in the Frome-Piddle catchment, Dorset, was supported by the Natural Environment
522 Research Council (algorithm studentship awarded to Grieg Davies) and Queen Mary University of
523 London (through a College studentship awarded to Bob Grabowski).

524 **References**

- 525 Adhitya, A., T. Bouma, A. Folkard, M. van Katwijk, D. Callaghan, H. de Iongh, and P. Herman.
526 2014. Comparison of the influence of patch-scale and meadow-scale characteristics on flow
527 within seagrass meadows: a flume study. *Marine Ecology Progress Series* **516**: 49-59.
- 528 Akaike, H. 1998. Information theory and an extension of the maximum likelihood principle, p. 199-
529 213. *Selected Papers of Hirotugu Akaike*. Springer.
- 530 Ashraf, I., H. Bradshaw, T.-T. Ha, J. Halloy, R. Godoy-Diana, and B. Thiria. 2017. Simple phalanx
531 pattern leads to energy saving in cohesive fish schooling. *Proceedings of the National*
532 *Academy of Sciences* **114**: 9599-9604.

533 Bal, K. D., T. J. Bouma, K. Buis, E. Struyf, S. Jonas, H. Backx, and P. Meire. 2011. Trade-off between
534 drag reduction and light interception of macrophytes: comparing five aquatic plants with
535 contrasting morphology. *Functional Ecology* **25**: 1197-1205.

536 Balke, T., T. J. Bouma, E. M. Horstman, E. L. Webb, P. L. Erftemeijer, and P. M. Herman. 2011.
537 Windows of opportunity: thresholds to mangrove seedling establishment on tidal flats.
538 *Marine Ecology Progress Series* **440**: 1-9.

539 Balke, T., P. M. Herman, and T. J. Bouma. 2014. Critical transitions in disturbance-driven
540 ecosystems: identifying Windows of Opportunity for recovery. *Journal of Ecology* **102**: 700-
541 708.

542 Barrat-Segretain, M.-H., G. Bornette, and A. Hering-Vilas-Bôas. 1998. Comparative abilities of
543 vegetative regeneration among aquatic plants growing in disturbed habitats. *Aquatic Botany*
544 **60**: 201-211.

545 Barrat-Segretain, M.-H., C. P. Henry, and G. Bornette. 1999. Regeneration and colonization of
546 aquatic plant fragments in relation to the disturbance frequency of their habitats. *Archiv für*
547 *Hydrobiologie* **145**: 111-127.

548 Bertoldi, W., M. Welber, A. Gurnell, L. Mao, F. Comiti, and M. Tal. 2015. Physical modelling of the
549 combined effect of vegetation and wood on river morphology. *Geomorphology* **246**: 178-
550 187.

551 Bill, R. G., and W. F. Herrnkind. 1976. Drag reduction by formation movement in spiny lobsters.
552 *Science* **193**: 1146-1148.

553 Bouma, T., M. De Vries, E. Low, G. Peralta, I. Tánčzos, J. van de Koppel, and P. J. Herman. 2005.
554 Trade-offs related to ecosystem engineering: A case study on stiffness of emerging
555 macrophytes. *Ecology* **86**: 2187-2199.

556 Bouma, T., M. Friedrichs, B. Van Wesenbeeck, S. Temmerman, G. Graf, and P. Herman. 2009.
557 Density-dependent linkage of scale-dependent feedbacks: A flume study on the intertidal
558 macrophyte *Spartina anglica*. *Oikos* **118**: 260-268.

559 Bouma, T., L. Van Duren, S. Temmerman, T. Claverie, A. Blanco-Garcia, T. Ysebaert, and P. Herman.
560 2007. Spatial flow and sedimentation patterns within patches of epibenthic structures:
561 Combining field, flume and modelling experiments. *Continental Shelf Research* **27**: 1020-
562 1045.

563 Bruno, J. F., and C. W. Kennedy. 2000. Patch-size dependent habitat modification and facilitation on
564 New England cobble beaches by *Spartina alterniflora*. *Oecologia* **122**: 98-108.

565 Bruno, J. F., J. J. Stachowicz, and M. D. Bertness. 2003. Inclusion of facilitation into ecological
566 theory. *Trends in Ecology & Evolution* **18**: 119-125.

567 Callaway, R. M. 2007. Direct Mechanisms for Facilitation, p. 15-116. *Positive Interactions and*
568 *Interdependence in Plant Communities*. Springer Netherlands.

569 Cameron, S. M., V. I. Nikora, I. Albayrak, O. Miler, M. Stewart, and F. Siniscalchi. 2013. Interactions
570 between aquatic plants and turbulent flow: a field study using stereoscopic PIV. *Journal of*
571 *Fluid Mechanics* **732**: 345-372.

572 Chen, Z., C. Jiang, and H. Nepf. 2013. Flow adjustment at the leading edge of a submerged aquatic
573 canopy. *Water Resources Research* **49**: 5537-5551.

574 Chen, Z., A. Ortiz, L. Zong, and H. Nepf. 2012. The wake structure behind a porous obstruction and
575 its implications for deposition near a finite patch of emergent vegetation. *Water Resources*
576 *Research* **48**: W09517.

577 Corenblit, D., A. Baas, T. Balke, T. Bouma, F. Fromard, V. Garófano-Gómez, E. González, A. M.
578 Gurnell, B. Hortobágyi, and F. Julien. 2015. Engineer pioneer plants respond to and affect

579 geomorphic constraints similarly along water–terrestrial interfaces world-wide. *Global*
580 *Ecology and Biogeography* **24**: 1363-1376.

581 Corenblit, D., E. Tabacchi, J. Steiger, and A. M. Gurnell. 2007. Reciprocal interactions and
582 adjustments between fluvial landforms and vegetation dynamics in river corridors: a review
583 of complementary approaches. *Earth-Science Reviews* **84**: 56-86.

584 Cornacchia, L., S. Licci, H. Nepf, A. Folkard, D. van der Wal, J. van de Koppel, S. Puijalon, and T.
585 Bouma. 2018a. Turbulence-mediated facilitation of resource uptake in patchy stream
586 macrophytes. *Limnology and Oceanography*: doi:10.1002/lno.11070.

587 Cornacchia, L., J. Van De Koppel, D. Van Der Wal, G. Wharton, S. Puijalon, and T. J. Bouma. 2018b.
588 Landscapes of facilitation: how self-organized patchiness of aquatic macrophytes promotes
589 diversity in streams. *Ecology* **99**: 832-847.

590 Cotton, J., G. Wharton, J. Bass, C. Heppell, and R. Wotton. 2006. The effects of seasonal changes to
591 in-stream vegetation cover on patterns of flow and accumulation of sediment.
592 *Geomorphology* **77**: 320-334.

593 Davies, G. R. 2012. The transport and retention of fine sediments in seasonally vegetated lowland
594 streams. Queen Mary University of London.

595 Dawson, F. 1976. The annual production of the aquatic macrophyte *Ranunculus penicillatus* var.
596 *calcareus* (RW Butcher) C.D.K. Cook. *Aquatic Botany* **2**: 51-73.

597 ---. 1989. Ecology and management of water plants in lowland streams. In: Fifty-seventh annual
598 report for the year ended 31st March 1989. Ambleside, UK, Freshwater Biological
599 Association, pp. 43-60. (Annual Report, Freshwater Biological Association, Ambleside).

600 De Lima, P. H., J. G. Janzen, and H. M. Nepf. 2015. Flow patterns around two neighboring patches
601 of emergent vegetation and possible implications for deposition and vegetation growth.
602 *Environmental Fluid Mechanics* **15**: 881-898.

603 De Paoli, H. 2017. Restoring mussel beds: A guide on how to survive on an intertidal mudflat.
604 University of Groningen.

605 Folkard, A. M. 2005. Hydrodynamics of model *Posidonia oceanica* patches in shallow water.
606 Limnology and Oceanography **50**: 1592-1600.

607 ---. 2011. Flow regimes in gaps within stands of flexible vegetation: laboratory flume simulations.
608 Environmental Fluid Mechanics **11**: 289-306.

609 Fonseca, M. S., and S. S. Bell. 1998. Influence of physical setting on seagrass landscapes near
610 Beaufort, North Carolina, USA. Marine Ecology Progress Series: 109-121.

611 Grabowski, R. C., and A. Gurnell. 2016. Hydrogeomorphology—Ecology interactions in river
612 systems. River Research and Applications **32**: 139-141.

613 Gurnell, A. 2014. Plants as river system engineers. Earth Surface Processes and Landforms **39**: 4-25.

614 Gurnell, A., and R. Grabowski. 2016. Vegetation–hydrogeomorphology interactions in a low-energy,
615 human-impacted river. River Research and Applications **32**: 202-215.

616 Gurnell, A. M., M. T. O’Hare, J. M. O’Hare, P. Scarlett, and T. M. Liffen. 2013. The
617 geomorphological context and impact of the linear emergent macrophyte, *Sparganium*
618 *erectum* L.: a statistical analysis of observations from British rivers. Earth Surface Processes
619 and Landforms **38**: 1869-1880.

620 Haslam, S. M. 1978. River plants: the macrophyte vegetation of watercourses. Cambridge Univer.
621 Press. Cambridge.

622 Hendriks, I. E., T. Sintes, T. J. Bouma, and C. M. Duarte. 2008. Experimental assessment and
623 modeling evaluation of the effects of the seagrass *Posidonia oceanica* on flow and particle
624 trapping. Marine Ecology Progress Series.

625 Jaffe, M., and S. Forbes. 1993. Thigmomorphogenesis: the effect of mechanical perturbation on
626 plants. Plant Growth Regulation **12**: 313-324.

627 Jones, C. G., J. H. Lawton, and M. Shachak. 1994. Organisms as ecosystem engineers, p. 130-147.
628 Ecosystem management. Springer.

629 Kearney, W. S., and S. Fagherazzi. 2016. Salt marsh vegetation promotes efficient tidal channel
630 networks. *Nature Communications* **7**.

631 Kondziolka, J. M., and H. M. Nepf. 2014. Vegetation wakes and wake interaction shaping aquatic
632 landscape evolution. *Limnology and Oceanography: Fluids and Environments* **4**: 106-119.

633 Kouwen, N., and T. E. Unny. 1973. Flexible roughness in open channels. *Journal of the Hydraulics*
634 *Division* **99**.

635 Larsen, L. G., J. W. Harvey, and J. P. Crimaldi. 2007. A delicate balance: ecohydrological feedbacks
636 governing landscape morphology in a lotic peatland. *Ecological monographs* **77**: 591-614.

637 Leonard, L. A., and M. E. Luther. 1995. Flow hydrodynamics in tidal marsh canopies. *Limnology*
638 *and Oceanography* **40**: 1474-1484.

639 Liffen, T., A. Gurnell, and M. O'Hare. 2013. Profiling the below ground biomass of an emergent
640 macrophyte using an adapted ingrowth core method. *Aquatic botany* **110**: 97-102.

641 Lissaman, P., and C. A. Shollenberger. 1970. Formation flight of birds. *Science* **168**: 1003-1005.

642 Liu, Q.-X., P. M. Herman, W. M. Mooij, J. Huisman, M. Scheffer, H. Olf, and J. Van De Koppel.
643 2014. Pattern formation at multiple spatial scales drives the resilience of mussel bed
644 ecosystems. *Nature Communications* **5**.

645 Madsen, J. D., P. A. Chambers, W. F. James, E. W. Koch, and D. F. Westlake. 2001. The interaction
646 between water movement, sediment dynamics and submersed macrophytes. *Hydrobiologia*
647 **444**: 71-84.

648 Marjoribanks, T. I., R. J. Hardy, S. N. Lane, and M. J. Tancock. 2017. Patch-scale representation of
649 vegetation within hydraulic models. *Earth Surface Processes and Landforms* **42**: 699-710.

650 Meire, D. W., J. M. Kondziolka, and H. M. Nepf. 2014. Interaction between neighboring vegetation
651 patches: Impact on flow and deposition. *Water Resources Research* **50**: 3809-3825.

652 Murray, A., M. Knaapen, M. Tal, and M. Kirwan. 2008. Biomorphodynamics: Physical-biological
653 feedbacks that shape landscapes. *Water Resources Research* **44**: W11301.

654 Nepf, H., and E. Vivoni. 2000. Flow structure in depth-limited, vegetated flow. *Journal of*
655 *Geophysical Research: Oceans* **105**: 28547-28557.

656 Nepf, H. M. 2012. Flow and transport in regions with aquatic vegetation. *Annual Review of Fluid*
657 *Mechanics* **44**: 123-142.

658 Portugal, S. J., T. Y. Hubel, J. Fritz, S. Heese, D. Trobe, B. Voelkl, S. Hailes, A. M. Wilson, and J. R.
659 Usherwood. 2014. Upwash exploitation and downwash avoidance by flap phasing in ibis
660 formation flight. *Nature* **505**: 399-402.

661 Puijalon, S., T. J. Bouma, C. J. Douady, J. van Groenendael, N. P. Anten, E. Martel, and G. Bornette.
662 2011. Plant resistance to mechanical stress: evidence of an avoidance–tolerance trade-off.
663 *New Phytologist* **191**: 1141-1149.

664 Puijalon, S., J. P. Léna, N. Rivière, J. Y. Champagne, J. C. Rostan, and G. Bornette. 2008. Phenotypic
665 plasticity in response to mechanical stress: hydrodynamic performance and fitness of four
666 aquatic plant species. *New Phytologist* **177**: 907-917.

667 Rietkerk, M., M. C. Boerlijst, F. van Langevelde, R. HilleRisLambers, J. v. de Koppel, L. Kumar, H.
668 H. Prins, and A. M. de Roos. 2002. Self-organization of vegetation in arid ecosystems. *The*
669 *American Naturalist* **160**: 524-530.

670 Rietkerk, M., and J. Van de Koppel. 2008. Regular pattern formation in real ecosystems. *Trends in*
671 *ecology & evolution* **23**: 169-175.

672 Riis, T. 2008. Dispersal and colonisation of plants in lowland streams: success rates and bottlenecks.
673 *Hydrobiologia* **596**: 341-351.

674 Riis, T., and B. J. Biggs. 2003. Hydrologic and hydraulic control of macrophyte establishment and
675 performance in streams. *Limnology and oceanography* **48**: 1488-1497.

676 Sand-Jensen, K. 1998. Influence of submerged macrophytes on sediment composition and near-bed
677 flow in lowland streams. *Freshwater Biology* **39**: 663-679.

678 Sand-Jensen, K., and J. R. Mebus. 1996. Fine-scale patterns of water velocity within macrophyte
679 patches in streams. *Oikos* **76**: 169-180.

680 Sand-Jensen, K., and T. Vindbæk Madsen. 1992. Patch dynamics of the stream macrophyte,
681 *Callitriche cophocarpa*. *Freshwater Biology* **27**: 277-282.

682 Sand-Jensen, K., K. Andersen, and T. Andersen. 1999. Dynamic properties of recruitment, expansion
683 and mortality of macrophyte patches in streams. *International Review of Hydrobiology* **84**:
684 497-508.

685 Schoelynck, J., T. De Groote, K. Bal, W. Vandenbruwaene, P. Meire, and S. Temmerman. 2012. Self-
686 organised patchiness and scale-dependent bio-geomorphic feedbacks in aquatic river
687 vegetation. *Ecography* **35**: 760-768.

688 Schutten, J., J. Dainty, and A. Davy. 2005. Root anchorage and its significance for submerged plants
689 in shallow lakes. *Journal of Ecology* **93**: 556-571.

690 Tal, M., and C. Paola. 2007. Dynamic single-thread channels maintained by the interaction of flow
691 and vegetation. *Geology* **35**: 347-350.

692 Temmerman, S., T. Bouma, J. Van de Koppel, D. Van der Wal, M. De Vries, and P. Herman. 2007.
693 Vegetation causes channel erosion in a tidal landscape. *Geology* **35**: 631-634.

694 Van de Koppel, J., J. C. Gascoigne, G. Theraulaz, M. Rietkerk, W. M. Mooij, and P. M. Herman.
695 2008. Experimental evidence for spatial self-organization and its emergent effects in mussel
696 bed ecosystems. *Science* **322**: 739-742.

697 van de Koppel, J., M. Rietkerk, N. Dankers, and P. M. Herman. 2005. Scale-dependent feedback and
698 regular spatial patterns in young mussel beds. *The American Naturalist* **165**: E66-E77.

699 Van der Wal, D., A. Wielemaker-Van den Dool, and P. M. Herman. 2008. Spatial patterns, rates and
700 mechanisms of saltmarsh cycles (Westerschelde, The Netherlands). *Estuarine, Coastal and*
701 *Shelf Science* **76**: 357-368.

702 van Wesenbeeck, B. K., J. Van De Koppel, P. MJ Herman, and T. J Bouma. 2008. Does scale-
703 dependent feedback explain spatial complexity in salt-marsh ecosystems? *Oikos* **117**: 152-
704 159.

705 Vandenbruwaene, W., S. Temmerman, T. Bouma, P. Klaassen, M. De Vries, D. Callaghan, P. Van
706 Steeg, F. Dekker, L. Van Duren, and E. Martini. 2011. Flow interaction with dynamic
707 vegetation patches: Implications for biogeomorphic evolution of a tidal landscape. *Journal*
708 *of Geophysical Research: Earth Surface* **116**.

709 Weimerskirch, H., J. Martin, Y. Clerquin, P. Alexandre, and S. Jiraskova. 2001. Energy saving in
710 flight formation. *Nature* **413**: 697-698.

711 Wharton, G., J. A. Cotton, R. S. Wotton, J. A. Bass, C. M. Heppell, M. Trimmer, I. A. Sanders, and
712 L. L. Warren. 2006. Macrophytes and suspension-feeding invertebrates modify flows and
713 fine sediments in the Frome and Piddle catchments, Dorset (UK). *Journal of Hydrology* **330**:
714 171-184.

715 Zong, L., and H. Nepf. 2011. Spatial distribution of deposition within a patch of vegetation. *Water*
716 *Resources Research* **47**: W03516.

717 ---. 2012. Vortex development behind a finite porous obstruction in a channel. *Journal of Fluid*
718 *Mechanics* **691**: 368-391.

720 **Table 1** Regression results of linear and quadratic models including single (T, L) or multiple (T and
 721 L) predictor variables. Final selected models (in bold) are based on Akaike Information Criterion
 722 (AIC) values.

	<i>Linear model</i>			<i>Quadratic model</i>			
	Predictor variables						
	T * L	T	L	T * L	T	L	
Relative \bar{U} between patches	R ²	0.82	0.79	0.00	0.87	0.81	0.06
	p-value	0.01	0.0005	0.84	0.058	0.002	0.79
	AIC	-17.64	-19.96	-4.06	-16.99	-19.08	-2.67
Relative \bar{U} upstream of patch “D”	R ²	0.40	0.24	0.05	0.71	0.33	0.28
	p-value	0.33	0.15	0.49	0.26	0.24	0.31
	AIC	-6.22	-7.71	-5.59	-9.37	-7.05	-6.28
Relative \bar{U} next to patch “U”	R ²	0.41	0.22	0.00	0.90	0.25	0.69
	p-value	0.329	0.16	0.99	0.033	0.36	0.016
	AIC	-25.53	-26.77	-24.19	-40.09	-25.10	-33.95
Relative \bar{U} next to patch “D”	R ²	0.33	0.31	0.00	0.38	0.31	0.085
	p-value	0.45	0.09	0.95	0.76	0.26	0.73
	AIC	-22.32	-26.05	-22.29	-19.15	-24.05	-21.18
TKE upstream of patch “D”	R ²	0.31	0.00	0.27	0.76	0.07	0.62
	p-value	0.48	0.99	0.11	0.18	0.77	0.03
	AIC	-80.09	-80.31	-83.53	-86.83	-79.04	-87.99

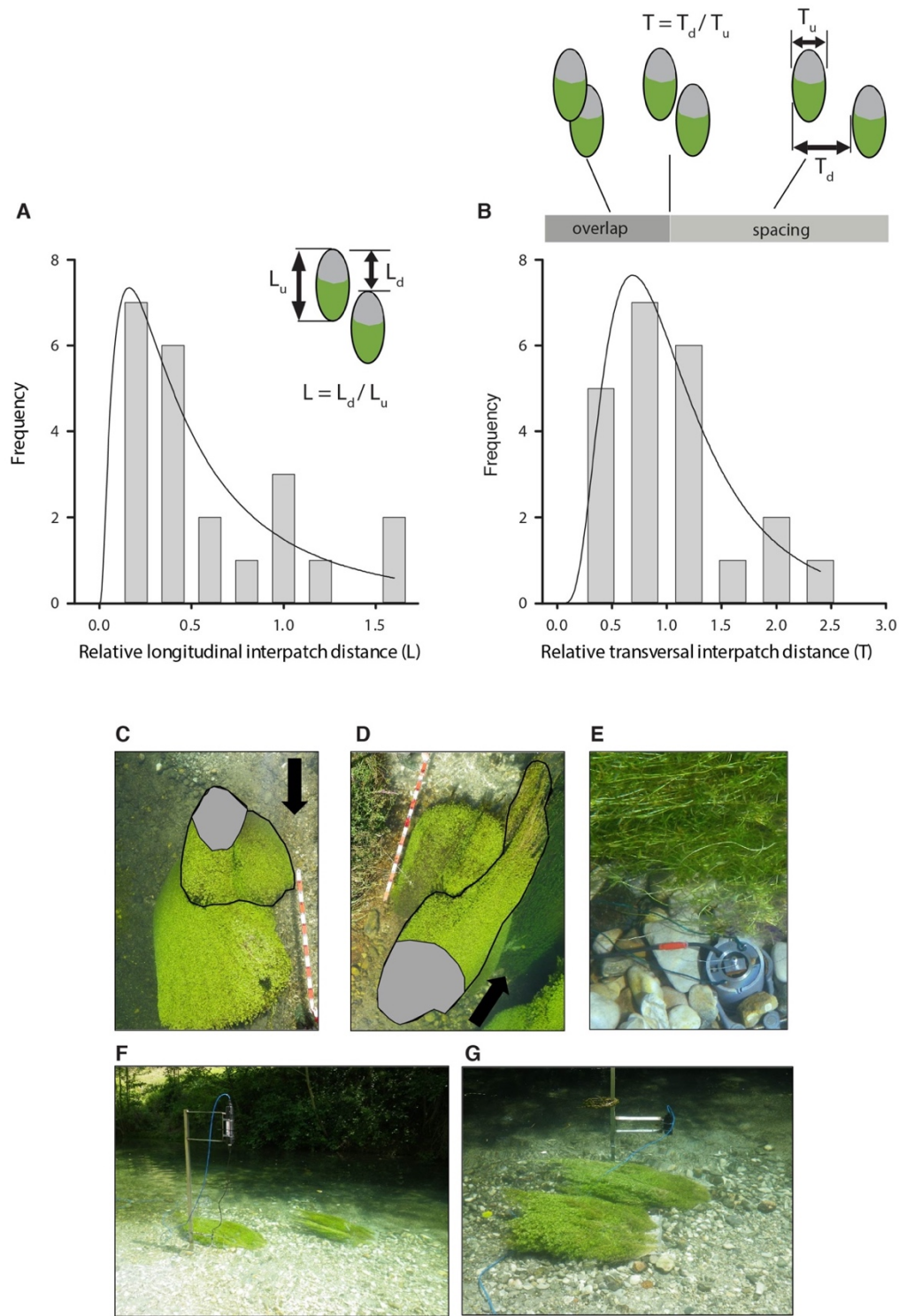
723

724

725 **Table 2** Changes in *Ranunculus* in-stream vegetation cover (%) and direction of growth of newly
 726 occurring vegetation patches with respect to the nearest existing vegetation patch (°), based on field
 727 observations in the Frome-Piddle catchment (UK), performed over three different time periods
 728 covering the annual growth cycle. Observations were of the dominant species *Ranunculus*
 729 *penicillatus* subsp. *pseudofluitans*.

		Dec. 2008	July 2009	Sept. 2009	Jan. 2010	July 2010
<i>Ranunculus</i> cover (%)		13	22	7	22	30
Angle to nearest vegetation patch (°)		Dec. 08 – July 09	Sept. 09 – Jan. 10	Jan. 10 – July 10	Total	
Downstream	0 – 60	5	5	6	16	
	60 – 120	0	3	1	4	
	120 – 180	3	2	4	9	
Upstream	180 – 240	1	0	5	6	
	240 – 300	1	0	0	1	
	300 – 360	1	0	1	2	
Total		11	10	17	38	
χ^2		9.20	12.80	10.88	24.34	
d.f.		5	5	5	5	
p- value		0.1	0.025	0.053	< 0.001	

730

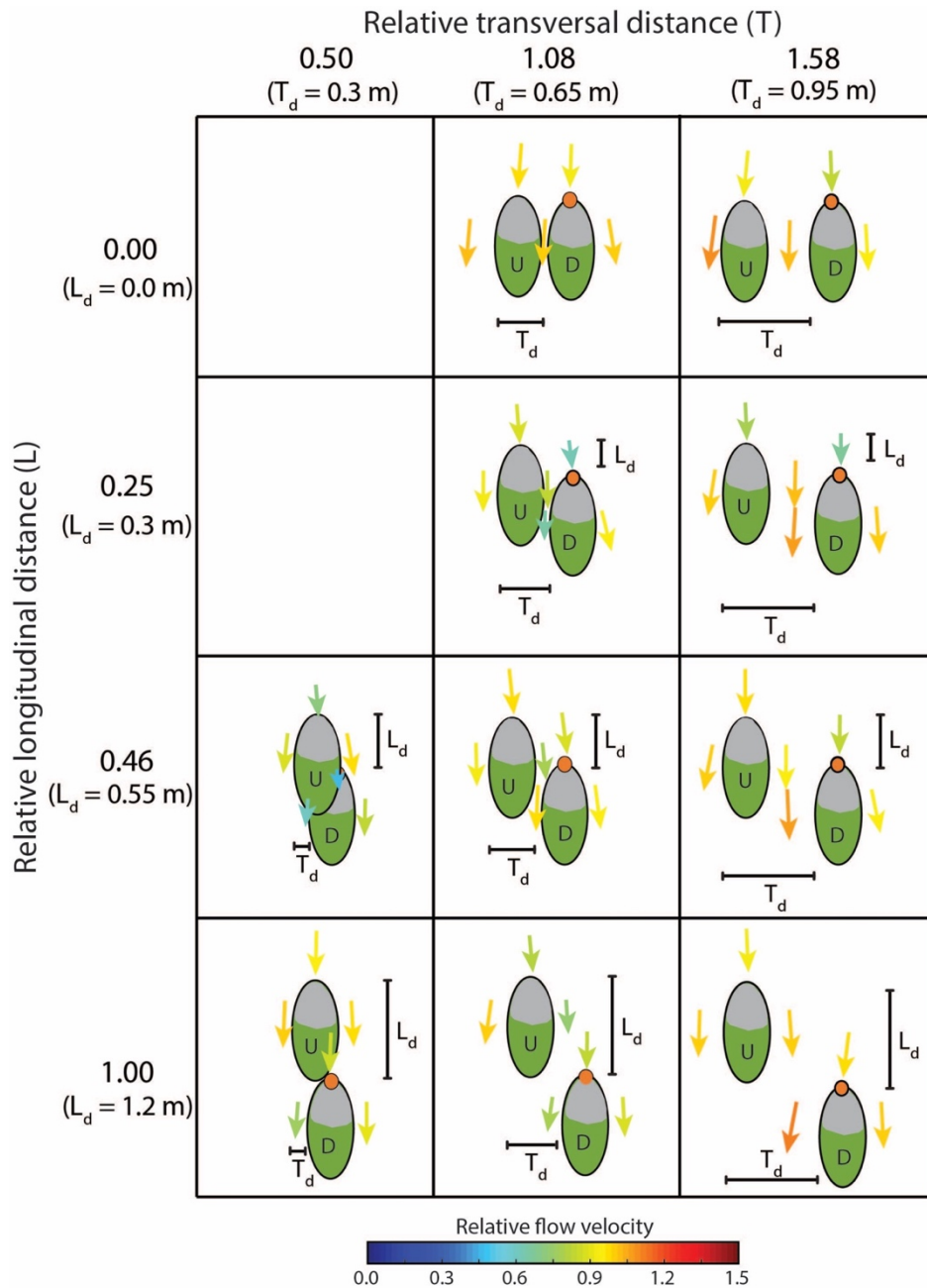


732

733 **Figure 1** Frequency distribution of A) observed relative longitudinal inter-patch distance (distance

734 between upstream edges divided by upstream patch length) and B) relative transversal interpatch

735 distance (transversal gap between leftmost edges divided by upstream patch width) of neighbouring
736 patches of *Callitriche platycarpa*. The aerial pictures show macrophyte patch pairs (C, D) growing
737 in a staggered distribution, with overlapping canopies. The canopy of the upstream patch is outlined
738 in black. Grey areas indicate the extent of the rooted area. Arrows indicate main river flow
739 direction. E shows the force transducer employed in the field for drag measurements on
740 macrophytes. F and G illustrate the experimental setup in the field with the transplanted vegetation
741 patches and ADV for flow velocity measurements.



742

743 **Figure 2** Overview of the ten patch configurations used in the field experiments, with indication of

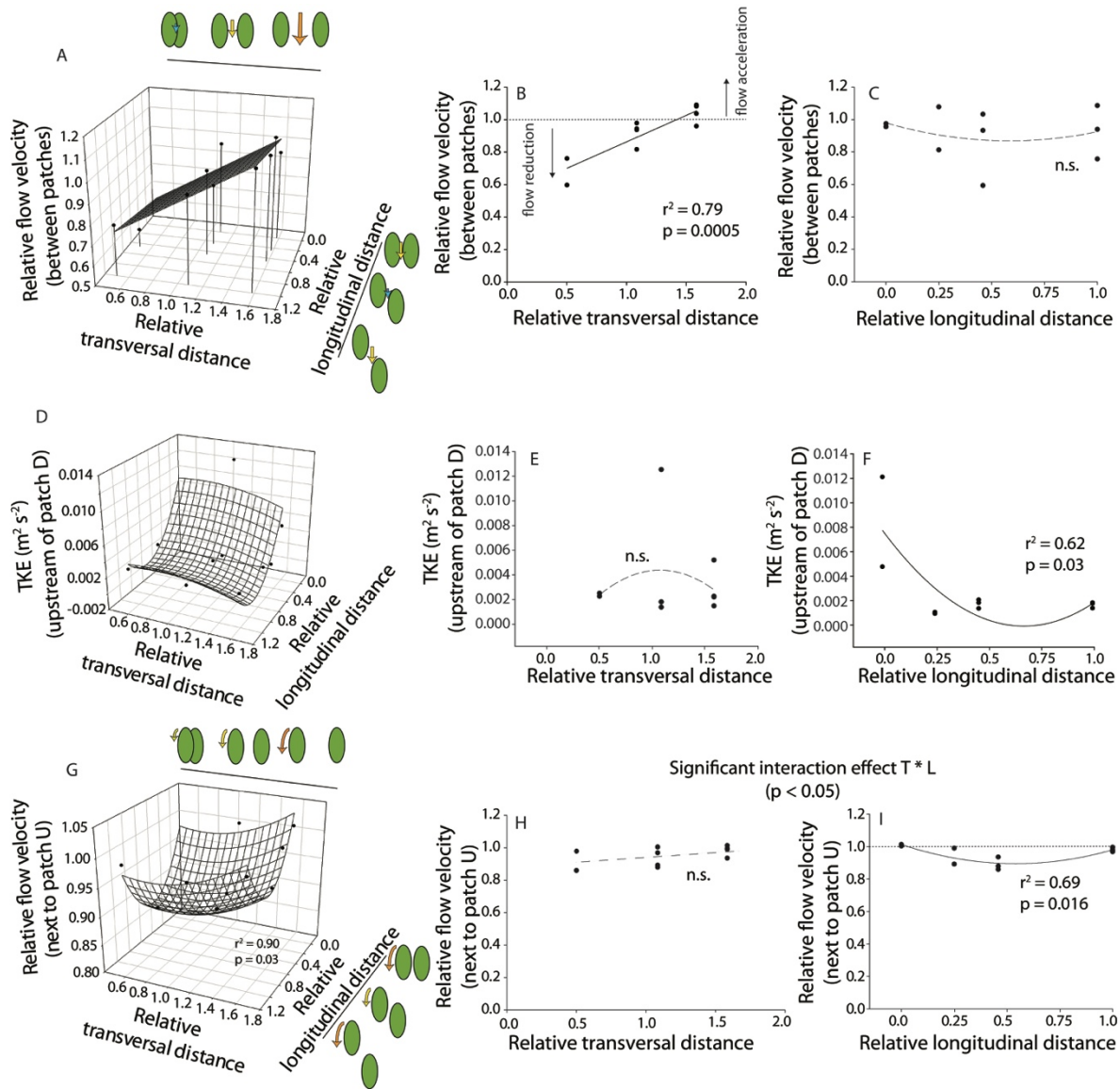
744 inter-patch distance in the longitudinal and transversal directions. L and T are relative distances; T_d

745 and L_d are absolute distances (in m). Patch “U” was kept fixed, while patch “D” was moved

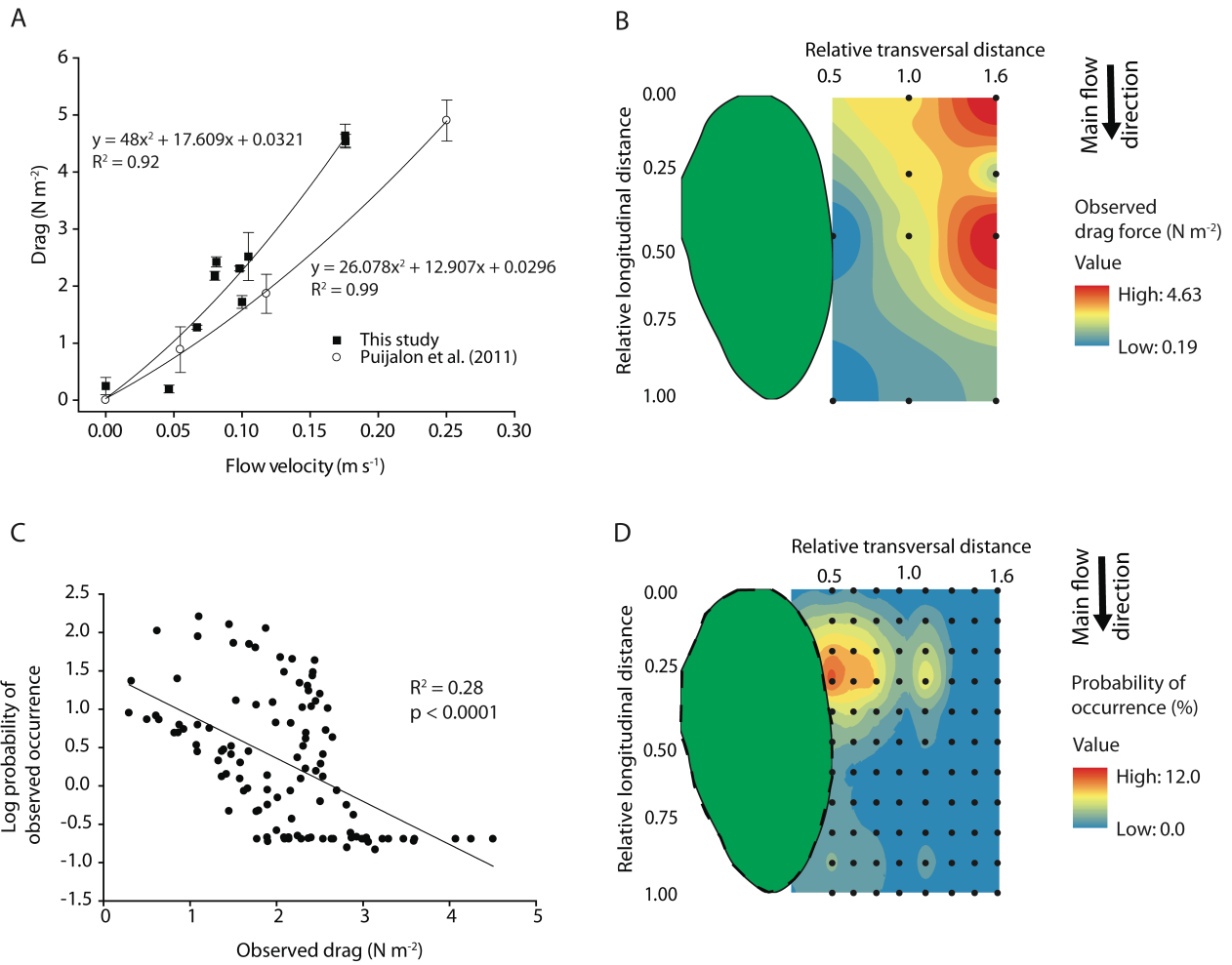
746 downstream and/or laterally. Arrows indicate flow direction, and arrow size and colour indicate

747 velocity magnitude relative to a measurement point located 0.5 m upstream of patch U. Grey areas

748 indicate the extent of the rooted area. Orange dots are locations of drag measurements.



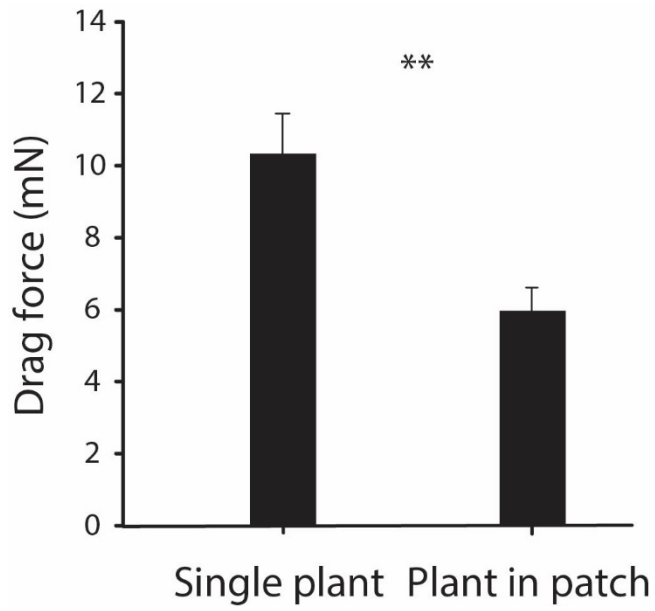
749
 750 **Figure 3** Relative flow velocity measurements (flow velocity relative to incoming flow) in between
 751 the patches (A, B, C) and on the side of patch U (G, H, I) for the ten configurations, showing the
 752 effects of increasing relative longitudinal and transversal distances. (D, E, F) Relationship between
 753 relative longitudinal and transversal distances and turbulent kinetic energy (TKE, $m^2 s^{-2}$) at the
 754 upstream edge of patch D. Green ovals are illustrations of the two neighbouring patches and their
 755 relative separation distances on the axes. Arrow size and colour indicate flow velocity magnitude,
 756 according to the colour scale in Figure 2.



757

758 **Figure 4 (A – B)** Drag forces per unit surface area on single *C. platycarpa* individuals in different
 759 positions around a vegetation patch in the field flume. In A, relationship between flow velocity and
 760 drag force in the field (this study) and in a laboratory flume (Puijalon et al., 2011). In B, the drag
 761 measurements (black dots, same points as in A) are plotted in an interpolated spatial grid around an
 762 existing vegetation patch (in green). (C – D) Probability of observed patch occurrence around an
 763 existing vegetation patch. In C, spatial regression between the experimental drag in a certain
 764 position around a vegetation patch, and the probability of patch occurrence in the same position. In
 765 D, map of probability of patch occurrence (%), based on the combination of the observed frequency
 766 distributions of relative longitudinal and transversal distances in Figure 1. Black dots indicate the

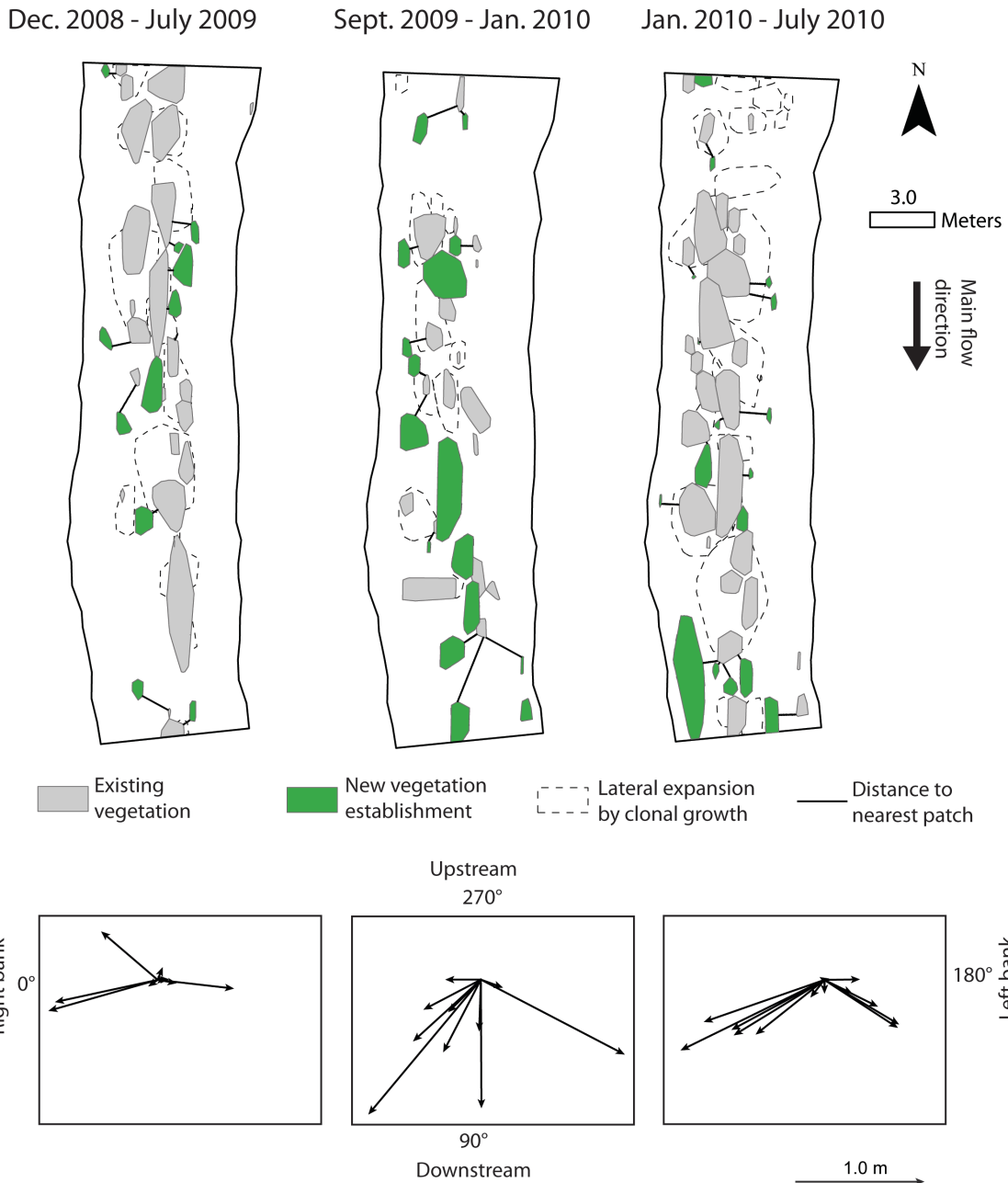
767 grid of distance observations. Note that the vegetation patch (green oval with dashed line border)
768 provides an indication of the average size of an existing patch; the actual size observed in natural
769 neighbouring patches may vary.



770

771 **Figure 5** Drag forces on a single plant vs. a plant located in a vegetation patch, averaged over the
772 ten vegetation configurations (paired t-test, $t_{19} = -2.2813$, $p = 0.03$). Error bars indicate standard
773 error.

774



775
 776 **Figure 6** Top: Planform representation of the distribution of in-stream macrophyte patches of
 777 *Ranunculus penicillatus* subsp. *pseudofluitans*. In grey: existing vegetation patches at the start of
 778 the survey period; dotted lines: lateral expansion of initial vegetation patches through clonal
 779 growth; in green: new patches occurring at the end of the survey period. Black lines indicate the
 780 shortest distance and direction of growth between the newly occurring vegetation and the nearest

781 existing patch. *Bottom*: distance and direction of growth (°) of new vegetation patches in each time
782 period over the stream bed.